TRACKING GRAZING PRESSURE AND CLIMATE INTERACTION - THE ROLE OF LANDSAT FRACTIONAL COVER IN TIME SERIES ANALYSIS

Peter Scarth[1], Achim Röder[2] and Michael Schmidt[3]

28th March 2011

[1] *Joint Remote Sensing Research Program*
Remote Sensing Centre, Queensland Department of Environment and Resource Management, 80 Meiers Road, Indooroopilly, QLD 4068, Australia
Centre for Spatial Environmental Research, School of Geography, Planning and Environmental Management, The University of Queensland, Brisbane, QLD 4072, Australia
[2] *Universität Trier FB VI Geography/Geosciences Remote Sensing Department Campus II D-54286 Trier*
[3] *Remote Sensing Centre, Queensland Department of Environment and Resource Management, 80 Meiers Road, Indooroopilly, QLD 4068, Australia*
Ph: +61 7 3896 9627
Email: peter.scarth@qld.gov.au

Abstract

Over 60% of Queensland's land area is classified as rangeland, areas which are subject to high climatic variability and are primarily devoted to grazing by cattle and other herbivores. Graziers, industry and governments require rangeland land condition data at appropriate spatial and temporal scales for sustainable economic and environmental management, to monitor changes in land condition and fulfil reporting obligations. A large body of work has been undertaken in Australian rangelands studying the relationship between satellite images and field measured vegetation cover leading to several operational monitoring programs. One such program is the Queensland Department of Environment and Resource Management's groundcover monitoring system that routinely produces fractional cover estimates across Queensland and New South Wales.

However, the interaction between climate and management in rangeland environments complicates the interpretation of data on condition and trend. One of the most promising methods to identify cycles and long term trends in rangelands is to examine time sequences of satellite images. Access to the United States Geological Survey (USGS) Landsat image archive affords an unprecedented number of images for use in both research and operational monitoring, permitting the effects of climate and management to be decoupled.

This work reports on the results of a time series analysis based on 15 years of monthly Landsat derived fractional cover over an intensively studied grazing trial in North Queensland. A number of rangeland condition indicators are examined, including vegetation cover and type and their trends and transitions due to climate and management. The results demonstrate a clear link between grazing pressure and the resilience of the grazing resource in the presence of climate variability at the intrinsic temporal and spatial scales at which changes occur in the system. The results highlight the importance of adaptable land management strategies and are being used to inform landholders, regional bodies and policymakers on state scale rangeland condition and trend.

1 Introduction

1.1 Rangelands

Rangelands are those areas where the rainfall is too low or unreliable and the soils too poor to support regular cropping. This definition covers about 81% of Australia and includes diverse savannas, woodlands, shrublands, grasslands and wetlands. Rangelands provide substantial benefits to Australia, including production of agricultural commodities, mineral extraction, the use of natural resources such as water for a range of purposes, and cultural values fundamental to Indigenous Australians (Bastin, 2008). Rangelands provide substantial economic benefits to the broader community, including much of Australia's mineral wealth (~$12 billion/year), income from sheep and cattle ($1.8 billion in 2001), other non-pastoral agriculture ($627 million in 2001) and income

from tourism estimated to exceed $2 billion (Bastin, 2008). Rangelands are subject to high climate variability on seasonal, annual, decadal and longer timescales making management for economic and environmental sustainability difficult. The sustainable management of rangelands would be better facilitated by easy access to broad scale objective information concerning rangeland condition and trend over time, but the impacts of climate and management interact to complicate interpretation of data on rangeland condition (Hill et al., 2005), problems that cannot be solved through simple aggregation since monitoring information on land condition and trend is required at management-relevant scales (Wallace et al., 2006). These issues of inadequate spatial coverage and temporal variability can be overcome by the use of time-series remote sensing data which provide a quantitative method to consistently identify temporal changes in rangeland vegetation at multiple spatial scales.

1.2 Remote Sensing

Landsat imagery, which offers a consistent broad scale monitoring ability, is ideally suited to monitoring the vast areas of Australian rangelands, where underlying trends in land condition affected by climatic variability may operate over periods of a decade or more (Pickup et al., 1998). The Landsat satellite image archive extends back to 1972 and is unmatched in quality, detail and coverage (Williams et al., 2006). A large body of work has been undertaken in Australian rangelands over the last 25 years, studying the relationships between reflected light recorded by Landsat satellites, and vegetation cover as measured at field sites (Bastin et al., 1998; Hassett et al., 2000; Hill and Kelly, 1986; Jafari et al., 2007; Ludwig et al., 2007; Pech et al., 1986a; Pickup et al., 1998; Scarth et al., 2006). For any modern rangeland monitoring system, there is now little doubt of the need for the extrapolative capacity of remote sensing technology combined with ground measurements and observations (Washington-Allen et al., 2006). But the process of mapping and monitoring land condition in rangelands has major challenges including system efficiencies in conducting monitoring over vast areas, separating management from natural seasonal effects, and deriving universal condition classes (Bastin and Ludwig, 2006). As result of these challenges there is still no definitive map of rangeland condition across the grazing lands of Queensland.

1.3 Groundcover

Groundcover in rangeland environments is variable in space and time, changing in response to both climatic variation and local pressure from grazing animals and anthropogenic influence such as cropping cycles, vegetation management and fire. In most natural systems, groundcover can be classified into either green, dead or bare cover. This classification problem allows a remote sensing mixture modelling approach to be used, where the pixel reflectance is assumed to be a linear combination of the proportional area of each cover type Garcia-Haro et al. (1996). There are many examples of spectral unmixing to look at groundcover components. Early work by Pech et al. (1986b) used image derived endmembers representing 'cover' and 'greenness' to map proportional cover types and landscape components across a rangeland. These methods were extended by Pickup et al. (1998) to look at grazing gradients and their changes over time. By extending the concept of groundcover in rangeland environments to include photosynthetic (green) vegetation, non-photosynthetic (dead) vegetation and bare soil, Harris and Asner (2003) showed how imaging spectroscopy can be used to detect fine scale spatial variations in cover that can be used to assess condition. By quantifying at the spatial and temporal variation in these components (Röder et al., 2007) developed an indirect indicator of land degradation. More recently variable endmember methods such as those used by (Roberts et al., 1998) have proved to be successful, particularly in complex urban environments. However these bundle methods fail in rangeland environments due to the similarity between senescent cover and bright soils (Asner and Heidebrecht, 2002), and and the similarity between shade and dark soil (Okin et al., 2001).

1.4 Monitoring

The Queensland Department of Environment and Resource Management (DERM) Remote Sensing Centre (RSC) produces a Landsat based groundcover index (Karfs et al., 2009) that can be applied to its standardised Landsat image archive (de Vries et al., 2007) to produce meaningful groundcover performance indicators. More recently, this work has been extended to produce fractional cover estimates (Schmidt et al., 2008). The interpretation of temporal fractional cover changes in rangelands is difficult, however recent work has extended calibration across different sensor types (Röder et al., 2005), improved grazing gradient methodologies (Röder et al., 2007) and has developed techniques to monitor dynamic landcover and rangeland processes (Röder et al., 2008a,b).

1.5 Mixture Models

Fractional cover methods rely on having a good spectral library where the spectra is collected either in the field spectrometer or from the image itself. The term "endmember" assumes that it is a pure component, so

in the case of groundcover a pure bare component has to be pure bare soil, a pure green component contains entirely green plant material and a dead component is 100% dead leaves, senescent vegetation and/or litter with no soil background visible. It is rare to find a pure 30m x 30m Landsat pixel in heterogeneous rangeland environment. Therefore, to characterise the inherent variability in rangeland environments it is necessary to develop methods to derive synthetic endmembers from field data representing impure pixels. It has been shown that a linear unmixing process is mathematically equivalent to multiple regression when an image index is derived by regressing the individual bands against field data (Puyou-Lascassies et al., 1994a; Settle and Campbell, 1998). Recent work has also shown that multiple regression techniques are very effective at estimating foliage cover across large spatial extents when the input calibration data represents the variability inherent in the landscape (Armston et al., 2009). This work seeks to use multiple regression of the field data against the image data to derive endmembers that can then be used within a constrained unmixing approach. Since the regression estimates represent an optimal estimator only in the training sites, we can use these endmember estimates within a constrained unmixing algorithm to provide a better estimate of the cover fractions outside the training regions.

1.6 Time Series

Analysis of time series imagery is often suggested to assist in the separation of climate from management in these rangeland systems (Washington-Allen et al., 2006). Several studies using time series analyses of factional cover indices have been undertaken in the Australian environment. These studies have used either AVHRR with NDVI as the cover surrogate (e.g. Lu et al., 2003) or MODIS with both NDVI and EVI as cover surrogates (e.g. Gill et al., 2009). One of the limitations of these approaches when applied to active grazing systems in dryland environments is the insensitivity of the green vegetation indices to the non-photosynthetic vegetative cover that is found in these areas. Previous work in dryland environments has demonstrated some success using green cover surrogates (e.g. Röder et al., 2008a; Stellmes et al., 2008) however for active monitoring systems it is desirable to proceed using methods that can work on both fractional bare ground and non photosynthetic vegetation (Karfs, 2009). This study will apply a time series decomposition to the fractional covers derived from Landsat data. This seasonal decomposition converts the time series signal into three components representing a trend, seasonal variation and the residual noise component. These component time series will be analysed on a paddock basis to determine the effects of different grazing strategies on cover components.

2 Data and Methods

2.1 Field Data

Field data was collected over several campaigns lasting from January 2000 until September 2009. Sites were selected based on an analysis of land types across Queensland, coupled with the expert knowledge of local field officers who pinpointed appropriate target sites. These sites were located in both homogeneous and heterogeneous environments across both grazing and cropping lands, and also sampled a range of overstorey tree canopies so that algorithms to remove the effect of tree canopies could be developed at a later stage. A map of field site location is shown in Figure1. The field survey method and the attributes collected are described in Scarth et al. (2006).

2.2 Image Data

Accurate detection and quantification of vegetation change over time and space requires removal of the confounding effects of geometric distortion, radiometric variability, illumination geometry, and cloud, shadow and water contamination from imagery. de Vries et al. (2007) details the RSC preprocessing methodology used in this work. To ensure consistency in the image time series, a cross calibration between Landsat TM and Landsat ETM+ was effected through the use of a multiple regression technique whereby two tandem scenes were precision rectified and then regressed against each other to come up with a multiple regression equation that converted the Landsat ETM+ radiance back to Landsat TM radiance. The blue band (Landsat band 1) was discarded in all the images due to the effects of Rayleigh scattering on shorter wavelengths. Signatures for Landsat bands 2 to 7 were extracted from a 3 x 3 pixel window surrounding the field site location using the method outlined in Scarth et al. (2006). Signatures were extracted from any image in the database where there was less then 60 days between the groundcover measurement and the image acquisition. The number of days between field and image data was used as a weighting in the regression since groundcover can change extremely rapidly after rainfall events or under heavy grazing conditions. A weighting was also used to account for variations in site heterogeneity, accounting for the fact that as the site heterogeneity increases, the certainty with which we can establish a mean cover value decreases (Korb et al., 2003). In all, 968 image signatures were extracted and used in the subsequent analysis.

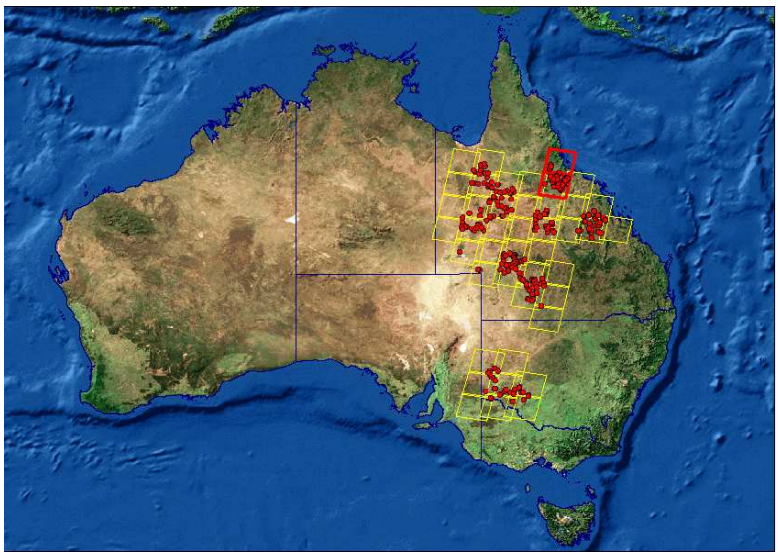

Figure 1: Map of Australia showing the location of field sample plots (red dots) and Landsat calibration scenes (yellow squares). The highlighted red Landsat scenes are where we have access to the full Landsat time series and represent the location of the field validation sites.

2.3 Generating Image Derived Endmembers

Settle (1996) examined the relationship between the "classical" and "inverse" models for estimating groundcover proportions, and showed that the difference between the two estimators is less than the prediction error when mixing is linear and signatures are well separated. The classical estimator is based on a physical linear mixture model that estimates the signal produced by a mixed pixel using a set of endmembers. Equation 1 has the multispectral signal x with b spectral bands modelled as a linear function of the c groundcover proportions f:

$$x = Mf + \epsilon \tag{1}$$

where M is a $(b \times c)$ matrix with c endmember spectra. The random noise term ϵ is assumed to be independent of f and to have zero mean. That is:

$$\varepsilon \sim N(0, \sigma^2 I) \tag{2}$$

where I is the identity matrix and σ^2 is the noise variance. This is one of the most widely used unmixing models and has been used in a large number of research and operational projects (e.g. Phinn et al., 2002; Röder et al., 2008b; Scarth and Phinn, 2000). It relies on the endmember spectra being linearly independent so that M is of full rank and invertible.

The inverse estimator relies on a linear regression of fractional groundcover against the multispectral signal and has also been applied successfully in many studies (e.g. Larsson, 1993; Williamson and Eldridge, 1993; Danaher et al., 2004; Fernandes et al., 2004). This estimator has the form of equation 3

$$f = Ax + a \tag{3}$$

where $(c \times b)$ matrix A and $(c \times 1)$ vector a are calculated from the training data using multivariate regression techniques (Kalivas, 1999). However this method relies on having a sufficiently variable training data set that adequately captures the landscape heterogeneity (Eldeiry et al., 2008; Salvador and Pons, 1998) and also requires that X, the $(b \times m)$ matrix of multispectral observations corresponding to the m field sites has sufficient rank to allow estimation of A (Xu, 1998). This inverse estimator has been shown to be a regularised form of the classical estimator under the assumption of linear mixing (Settle and Campbell, 1998).

The inverse estimator thus allows us to invert the field data set to derive a set of endmembers by regressing the Landsat data against the field data set and then inverting the multiple regression coefficients. Using this method, we can utilise many of the advantages of multiple regression models, such as including weighting in the regression relationship and allowing the inclusion of interactive terms that will assist in modelling nonlinearities within the system (Puyou-Lascassies et al., 1994b). The derived endmembers can then be used in a constrained mixture analysis to improve its ability to model areas outside the range of calibration.

2.3.1 Inverting The Field Observations

Given a field data represented as a $(c \times m)$ matrix F of field groundcover observations and X as the $([b+1] \times m)$ matrix of multispectral data, where the last row is a $(m \times 1)$ row of ones used to model the intercept vector a in equation 3, we can say:

$$F = AX \tag{4}$$

from which we can recover A using inversion techniques. The least square estimate is typically given as (Lawson, 1995):

$$A = (X^T X)^{-1} X^T F \tag{5}$$

In this work we use truncated singular value decomposition (Xu, 1998) so that the inversion can be performed in a lower-dimensional subspace, which is important if we are to attempt to model some of the nonlinearities using variable transforms. Denoting X^+ as the Moore–Penrose pseudoinverse, we can recover a least squares approximation to A by inversion of equation 4 as follows:

$$A \approx (X^+ F) \tag{6}$$

We can also incorporate weighting into equation 6 using the standard methods for least squares. If we have a weight vector w and define $X^{'} = wX$ and $F' = wF$ then equation 6 can be written as:

$$A \approx (X^{'+} F^{'}) \tag{7}$$

Since we are interested in using the classical estimator, from the analysis provided by Settle and Campbell (1998) we can compute the Moore–Penrose pseudoinverse A, obtained from equation 6 or equation 7 to obtain an estimate of M:

$$M \approx A^+ \approx (X^+ F)^+ \tag{8}$$

Note that this is a different result to inverting equation 1 directly so that:

$$M \approx X F^+ \tag{9}$$

since in this case we are assuming that the multispectral data is the independent variable. The validity and applicability of this estimate of the endmembers is highly dependent on having adequate field data that spans the range of cover amounts and their inherent spectral variability, and also relies on a judicious choice of subspace for the inversion (Elden, 2004). This estimate of the endmembers can then be used in a constrained unmixing model. It is important to note that unconstrained unmixing using the estimate of M is essentially identical to unmixing directly using equation 5. However we can use the estimate of M in a constrained approach which has significant advantages when a extrapolative ability is required.

2.3.2 Variable Transformation And Cross Validation

Some of the major difficulties encountered using simple linear unmixing are due to the presence of nonlinear effects which can cause model estimation errors. Since nonlinear spectral mixing occurs due to multiple reflection and transmission from surfaces it is particularly apparent in arid scenes where there is a bright background component, such as bright sandy soils and/or bright senescent vegetation (Okin et al., 2001; Ray and Murray, 1996). In the dry months, much of Queensland is covered in senescent vegetation and there are large tracts of very bright soils in the western regions resulting in considerable nonlinear mixing. In this work we account for mild nonlinearities by the inclusion of log transformed interactive components in the regression equations (Lawrence and Ripple, 1998) The use of the log transform helps to linearise multiplicative interactions. But one of the major problems when using interactive terms and transformed variables in models is the ease with which an over-fitted model may be created leading to artificially inflated results and large estimation errors when used outside its calibration (Salvador and Pons, 1998). Some common ways of dealing with this are by using stepwise regression methods where only the best explanatory subset variables are chosen (Grossman et al., 1996), or by subspace truncation methods such as principal component regression, partial least squares or ridge regression (Kalivas, 1999). This study used a subspace truncation method with the truncation value being chosen at the location of the lowest root mean square error (RMSE) point using a ten-fold cross validation approach.

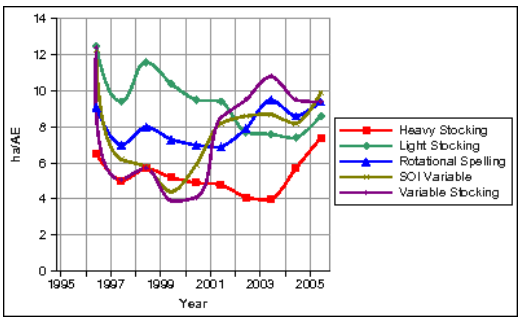

Figure 2: Wambiana grazing trial stocking rates for each of the five grazing strategies over the 1997 to 2005 trial period.

2.4 Unmixing Methodology

There are several different ways the classical estimator equation 1 can be specified to solve the inverse problem to recover the fractional amount of the endmember components from the spectral information in the pixel (Keshava and Mustard, 2002). In this work, we introduce constraints into the fractions such that $\sum_{i=1}^{c} f_i = 1$ (fractions must sum to 100%), and $f \geq 0$ (fractions are non-negative). Direct solutions are available for both the unconstrained equation and the sum to one constraint (Lawson, 1995). We solve the non-negative least squares (NNLS) problem using the iterative active set strategy proposed by Lawson and Hanson Lawson (1995). To solve for both constraints, we use the NNLS algorithm with a weighting strategy for the sum to one constraint that optimises the least squares error (Heinz and Chang, 2001). We do this by modifying equation 1 so that we solve:

$$\begin{bmatrix} x \\ \delta \end{bmatrix} = \begin{bmatrix} M \\ \delta 1^T \end{bmatrix} f + \epsilon \tag{10}$$

where δ is a weighting for the sum to one constraint and $1^T = \begin{bmatrix} 1 & 1 & \cdots & 1 \end{bmatrix}$ is a $c+1$ vector of ones. The optimal value of δ is determined during the 10-fold cross validation process.

2.4.1 Application To Imagery

The solution of equation 10 currently relies on the SciPy (Jones et al., 2001) wrapped version of the original FORTRAN nonlinear least squares routine by Lawson (1995). There is however a more efficient implementation of this routine and this will be used in future implementations to speed up the computation (Bro and Jong, 1997).

2.5 Wambiana Grazing Trial Data

The Wambiana grazing trial is located on Wambiana Station (20°34' S, 146°07' E), 70 km south-west of Charters Towers, north Queensland, Australia. Long-term mean annual precipitation is 636 mm but is highly seasonal, with most falling between December and March. This trial selected five grazing strategies for testing (heavy, light, variable, rotational and SOI variable) that were first stocked on 19 December 1997. Further details about the trial can be found in O'Reagain et al. (2009). Figure 2 shows the stocking rates for each of the strategies. Each grazing strategy was applied to two paddocks and the trial had 10 paddocks in total. The stocking rates vary over time, reflecting the climatic conditions experienced over this period. Field cover estimates were collected every six months over the 10 paddocks.

2.5.1 Time Series Fractional Cover At Wambiana

To test the performance of the fractional cover algorithm in a managed system, the unmixing model was applied to a time series of 189 Landsat TM and ETM+ images over the Wambiana field site. The mean cover value averaged across the entire paddock was compared with the mean of the field observed cover values after they had been transformed to objective cover estimates using the relationships from Murphy and Lodge (2002). Additionally, an seasonal decomposition (Schlicht, 1983) was performed on the time series to assess the relationship between the seasonal and trend fractional components and the grazing management strategies of the various paddocks.

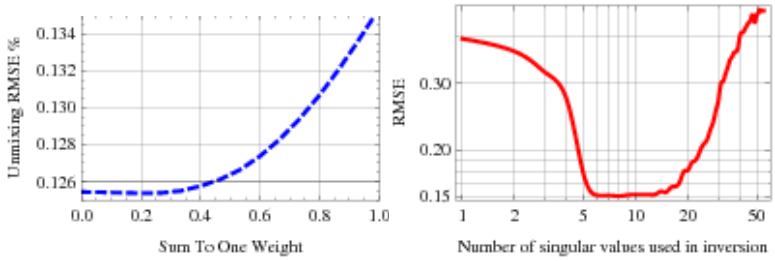

Figure 3: Left is 10 fold cross validation unmixing RMSE for the 968 field samples points vs. linear sum to one weight in the constrained unmixing model using endmembers derived using variable transformations. Right shows selection of optimal subspace by comparing the RMSE of the unmixing results in 10-Fold cross validation. Lowest RMSE occurs when 8 singular values are used in the model.

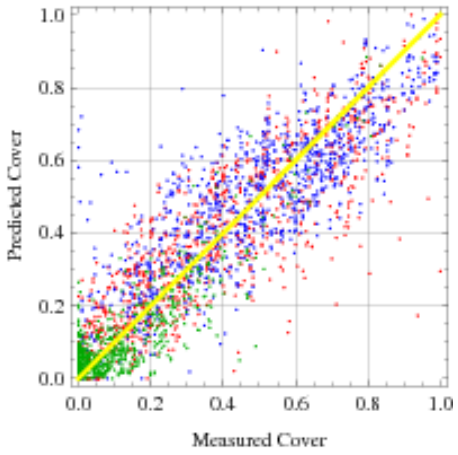

Figure 4: Unmixing results from the transformed model with interactive terms showing the fit of the bare (red), dead (blue) and green (green) components against the field determined values. This model had a RMSE of 11.8% and a $r^2$of 0.82 (t=36, p<0.01)

3 Results

3.1 Endmember Generation

The endmembers produced as a result of the inverse and classical equations in both spectral and transformed spectral space were initially visually checked from anomalies and then assessed against the field data for their modelling performance. The computation of interactive terms between all log transformed Landsat bands resulted in 55 synthetic spectral bands, many of which displayed a high level of correlation with other bands. It was therefore necessary to use cross validation to recover the optimal subspace and optimal sum to one constraint. It can be seen in Figure3 left that there is very little difference in the RMSE between an unconstrained model (sum to one weight equal to 0) and a sum to one constraint of the optimal value of 0.2. However it must be remembered that this is indicating that the unconstrained model fits the field data very well. When the model is being used in extrapolative sense is expected that the sum to one constraint becomes more important in constraining the range of values in the model solution to physically acceptable values. However it can be seen that constraint values higher than about 0.4 increase the error in the model significantly.

There is also a reasonably clear minima in Figure3 right highlighting the optimal number of singular values used in the inversion. The minimum unmixing RMSE is found when using 8 singular values although there is little difference in the root mean square error between eight and 13 singular values. This is significantly larger than the dimensionality of the original five band Landsat data and demonstrates that by adding interactive terms we are modelling some nonlinearities within the Landsat spectral subspace. It also displays the effects that come from over-fitting the problem when the dimensionality is increased beyond about 19.

The final model with the optimised to sum to one and subspace parameters is shown in Figure4. This final model has a root mean square error of 11.8% and a squared Pearson product moment correlation coefficient of 0.82. This result indicates that the model fits very well and the overall root mean square error, particularly in the mid-cover region, is improved over the current DERM groundcover model (Scarth et al., 2006).

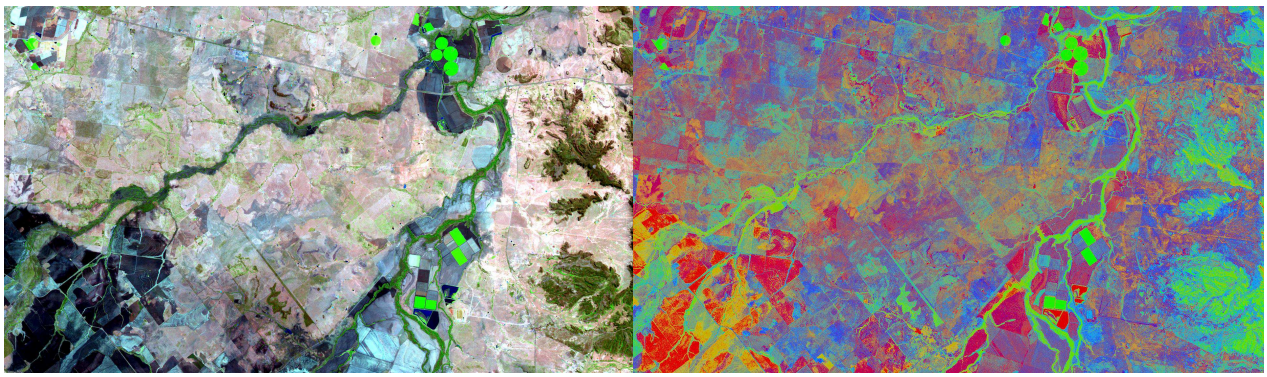

Figure 5: Left image is a 50 x 30km subset of a Landsat ETM+ scene near Emerald, Queensland in bands 5,4,3 as RGB and right, a fraction image of the same area with bare, green and dead as RGB.

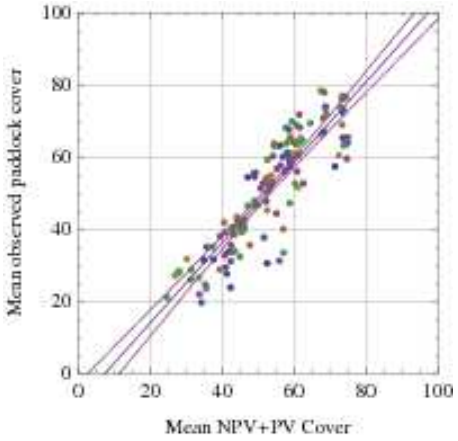

Figure 6: Comparison between field observed and satellite estimated cover. Coloured dots indicate the cover values from the 10 different paddocks in the trial. This model had a RMSE of 7.2% and a $r^2$of 0.78 (n=136, p=0.0000)

3.2 Fraction Images From The Constrained Model

The final model was applied to Landsat images across Queensland and the results were visually interpreted by operators with knowledge over these landscapes. Figure 5 shows an example heterogeneous landscape where there are extremely black dark cropping soils, crops growing in both paddock and centre pivot irrigation systems and areas of grazing and some natural woodland environments to the east of the image. The fraction image appears to accurately map the variation between the bare photosynthetic and non-photosynthetic components within the imagery. The active cropping, riparian and woodland areas are showing up clearly with a distinctive high photosynthetic response. The dark soils in the south-west of the scene are being displayed as highly bare although there is some evidence of a slight amount of green vegetation as indicated by some orange flecks in the fraction image. Towards the middle of the scene the variation in cover levels across different paddocks can be clearly seen. Image statistics indicate that there are no negative pixels and that 99.3% of all pixels within the image add up to 100%±10%.

3.3 Validation At Wambiana

3.3.1 Field Cover Estimates

Figure 6 shows the comparison between the field estimated cover values and the sum of the Landsat green and dead components measured over 10 paddocks at six monthly intervals. There is a strong and near linear 1:1 relationship with an RMSE of 7.2% . This result highlights the utility of satellite data to provide consistent, objective time series estimates that match what is observed on the ground.

3.3.2 Time Series Decomposition

In this work, we report on the seasonal decomposition applied to the heavily stocked and lightly stocked paddock time series. Several points are apparent in Figure 7. The key point is that there is clear separability

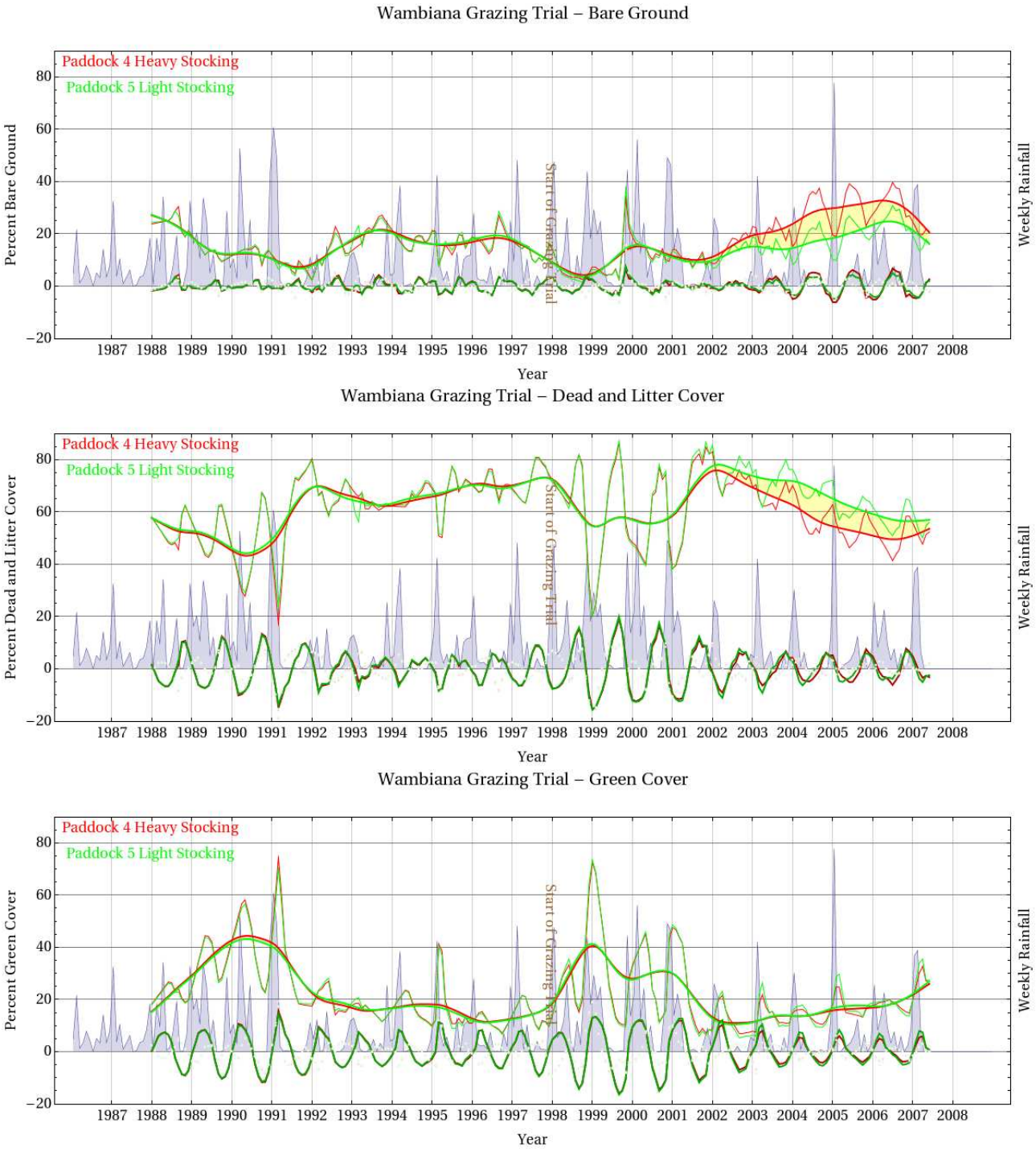

Figure 7: Plots of fractional cover time series over the heavy and light stocking rate paddocks on the Wambiana grazing trial following a seasonal decomposition. Upper plot is fractional bare ground, middle is fractional dead and litter cover and bottom plot is fractional green cover. Green and red lines represent the heavy and light stocking paddocks respectively. Thin lines are the raw Landsat time series, thick lines are the trend in the time series, darker lines are the seasonal component. Light dashed lines the the remaining "noise" component. Shaded light blue series represents weekly rainfall over the trial site. The start of the grazing trial in late 1997 is marked on each plot.

of the paddocks using either the trend of the bare ground or dead/litter fractions. The effect can be seen from 2002 onward, particularly as the drought across eastern Australia took hold. However, the difference in cover amounts due to the differing grazing strategies is only about 10%, indicating that in this environment climate has a larger impact on cover than the management strategies investigated in the trial. Also of interest is the slight but consistent phase difference, of the order of one month, in the dead and litter cover seasonal component during the trial. This is showing how the lightly grazed paddock is recovering considerably quicker after a rainfall event. Following significant rainfall, the dead/litter cover cyclic component drops very quickly in the lightly grazed paddock, indicating that this paddock is "greening-up" several weeks before the heavily grazed paddock. Further work will be required to ascertain if this effect is due to a greater number of perennial grasses in the lightly grazed paddock, or a greater remaining total standing dry matter (TSDM) amount at the end of the dry season.

The green cover fraction time series is clearly showing the effect of lagged vegetation response to rainfall in this environment. There is very little difference between the paddocks indicating that green cover is unrelated to stocking rate or management on Wambiana. Since the green fraction performs in a similar way to NDVI and other green vegetation indices, it is clear that these types of indices may be of little use in ascertaining management effects in these dry, seasonal environments. However, the green trend component has been steadily increasing since 2002. This counter-intuitive result (due to extreme drought conditions over this time) is due to the effects of a fire in late 1999. It has been reported that, following this fire event, the number of very small eucalypts approximately doubled through re-sprouting of top-killed individuals O'Reagain et al. (2009).

4 Conclusions And Future Work

This work has demonstrated how a network of field sites and imagery can be used to develop a robust statewide scale fractional cover model that successfully retrieves estimates of green, dead and bare ground fractions. By inverting the multiple linear regression estimates and using these synthetic endmembers in a constrained non-negative least squares unmixing model we have been able to successfully retrieve the groundcover fractions over a large number of scenes across Queensland and New South Wales, Australia.

Through the use of variable transforms and interactive terms, it has been possible to model a very wide range of different surface types with a simple three endmember model. This is convenient since we seek to use these estimates in time series analyses, so the use of a more complex model with a greater number of endmembers would require a rule-set to apportion the endmember fractions back to the green, dead and bare groundcover types. This work thus supports the work of Small (2004) by demonstrating that a three dimensional spectral mixing space is sufficient to model surface reflectance in many cases. Although successful in modelling a large range of groundcover types in Queensland and New South Wales, it is still not known how well this model would extrapolate across the complex and heterogeneous landscapes of Australia or indeed in other countries. Considerable validation effort is needed to establish the utility of fractional cover models across different landscapes; however it is often difficult to get synchronous field data with which to perform this type of validation. Future work will concentrate on collecting additional field data over a variety of different environments along with coincident imagery to continue the calibration and validation of these products. The physical mixture approach used in this work also allows the expansion of the model into different environments by using the additional spectral data to generate new model endmembers.

By using extensive field data sets to drive Landsat derived fractional cover time series, this work has improved methods to recover key indicators of rangeland condition, guiding better management decisions that lead to both environmental sustainability and economic productivity. Further work on cover time series derived from this research will work towards a greater understanding and spatialisation of the link between grazing pressure and the resilience of the grazing resource in the presence of considerable climate variability and climate change. These outputs benefit both local and national communities by delivering spatial information required by individual landholders, regional bodies, and Government reporting needs.

Acknowledgements

This work was performed while the author was on the Queensland international Fellowship with the University of Trier in Germany. We would like to than Peter O'Reagain and Grant Stone for background information and discussions about the Wambiana grazing trial. Sel Counter and the RSC team assisted in collecting the comprehensive field calibration and validation data. Geoscience Australia kindly provided the Landsat time series imagery for use in this research.

References

J. D. Armston, R. J. Denham, T. J. Danaher, P. F. Scarth, and T. N. Moffiet. Prediction and validation of foliage projective cover from Landsat-5 TM and Landsat-7 ETM+ imagery. *Journal of Applied Remote Sensing*, 3(1):033540–28, 2009.

G. P. Asner and K. B. Heidebrecht. Spectral unmixing of vegetation, soil and dry carbon cover in arid regions: Comparing multispectral and hyperspectral observations. *International Journal of Remote Sensing*, 23(19): 3939–3958, 2002.

G Bastin. *Rangelands 2008 - Taking the Pulse*. published on behalf of the ACRIS Management Committee by the National Land & Water Resources Audit, Canberra, 2008.

G. N. Bastin and J. A. Ludwig. Problems and prospects for mapping vegetation condition in Australia's arid rangelands. *Ecological Management and Restoration*, 7(SUPPL. 1), 2006.

G. N. Bastin, R. W. Tynan, and V. H. Chewings. Implementing satellite-based grazing gradient methods for rangeland assessment in South Australia. *Rangeland Journal*, 20(1):61–76, 1998.

R. Bro and S. de Jong. A fast non-negativity constrained least squares algorithm. *Journal of Chemometrics*, 11:393–401, 1997.

T. J. Danaher, J. D. Armston, and L. J. Collett. A multiple regression model for the estimation of woody foliage cover using Landsat in Queensland, Australia. *Proceedings of IGARSS 2004, Anchorage*, 2004.

C. de Vries, T. Danaher, R. Denham, P. Scarth, and S. Phinn. An operational radiometric calibration procedure for the Landsat sensors based on pseudo-invariant target sites. *Remote Sensing of Environment*, 107(3):414–429, 2007.

A.A. Eldeiry, L.A. Garcia, and R.M. Reich. Soil salinity sampling strategy using spatial modeling techniques, remote sensing, and field data. *Journal of Irrigation and Drainage Engineering*, 134(6):768–777, 2008. ISSN 07339437.

L. Elden. Partial least-squares vs. Lanczos bidiagonalization-I: Analysis of a projection method for multiple regression. *Computational Statistics and Data Analysis*, 46(1):11–31, 2004.

R. Fernandes, R. Fraser, R. Latifovic, J. Cihlar, J. Beaubien, and Y. Du. Approaches to fractional land cover and continuous field mapping: A comparative assessment over the BOREAS study region. *Remote Sensing of Environment*, 89(2):234–251, 2004.

F. J. Garcia-Haro, M. A. Gilabert, and J. Melia. Linear spectral mixture modelling to estimate vegetation amount from optical spectral data. *International Journal of Remote Sensing*, 17(17):3373–3400, 1996.

T. K. Gill, S. R. Phinn, J. D. Armston, and B. A. Pailthorpe. Estimating tree-cover change in Australia: Challenges of using the MODIS vegetation index product. *International Journal of Remote Sensing*, 30(6): 1547–1565, 2009.

Y. L. Grossman, S. L. Ustin, S. Jacquemoud, E. W. Sanderson, G. Schmuck, and J. Verdebout. Critique of stepwise multiple linear regression for the extraction of leaf biochemistry information from leaf reflectance data. *Remote Sensing of Environment*, 56(3):182–193, 1996.

A. T. Harris and G. P. Asner. Grazing gradient detection with airborne imaging spectroscopy on a semi-arid rangeland. *Journal of Arid Environments*, 55(3):391–404, 2003.

R.C. Hassett, H.L. Wood, J.O. Carter, and T.J. Danaher. A field method for statewide ground-truthing of a spatial pasture growth model. *Australian Journal of Experimental Agriculture*, 40(8):1069–1079, 2000.

D.C. Heinz and C.-I. Chang. Fully constrained least squares linear spectral mixture analysis method for material quantification in hyperspectral imagery. *IEEE Trans Geosci Remote Sens*, 39(3):529–545, 2001. ISSN 01962892 (ISSN).

G.J.E. Hill and G.D. Kelly. Integrating Landsat and land systems for cover maps in southern inland Queensland. *Australian Geographical Studies*, 24(2):235–243, 1986.

M. J. Hill, S. H. Roxburgh, J. O. Carter, and G. M. McKeon. Vegetation state change and consequent carbon dynamics in savanna woodlands of Australia in response to grazing, drought and fire: A scenario approach using 113 years of synthetic annual fire and grassland growth. *Australian Journal of Botany*, 53(7):715–739, 2005.

R. Jafari, M. M. Lewis, and B. Ostendorf. Evaluation of vegetation indices for assessing vegetation cover in southern arid lands in South Australia. *Rangeland Journal*, 29(1):39–49, 2007.

Eric Jones, Travis Oliphant, and Pearu Peterson. SciPy: Open Source Scientific Tools for Python, 2001.

J. H. Kalivas. Interrelationships of multivariate regression methods using eigenvector basis sets. *Journal of Chemometrics*, 13(2):111–132, 1999.

Abbott B.N. Scarth P.F. Wallace J.F. Karfs, R.A. Land condition monitoring information for Reef catchments: A new era. *Rangeland Journal*, 31(1):69–86, 2009. ISSN 10369872.

R. A. Karfs, B. N. Abbott, P. F. Scarth, and J. F. Wallace. Land condition monitoring information for reef catchments: a new era. *The Rangeland Journal*, 31(1):69–86, 2009.

N.a Keshava and J.F.b Mustard. Spectral unmixing. *IEEE Signal Processing Magazine*, 19(1):44–57, 2002. ISSN 10535888.

J. E. Korb, W. W. Covington, and P. Z. Fule. Sampling techniques influence understory plant trajectories after restoration: An example from ponderosa pine restoration. *Restoration Ecology*, 11(4):504–515, 2003.

H. Larsson. Linear regressions for canopy cover estimation in acacia woodlands using Landsat-TM, -MSS and SPOT HRV XS data. *International Journal of Remote Sensing*, 14(11):2129–2136, 1993.

R. L. Lawrence and W. J. Ripple. Comparisons among vegetation indices and bandwise regression in a highly disturbed, heterogeneous landscape: Mount St. Helens, Washington. *Remote Sensing of Environment*, 64(1): 91–102, 1998.

Charles L. Lawson. *Solving least squares problems*. Classics in applied mathematics : 15. Siam, Philadelphia, 1995.

H. Lu, M.R. Raupach, T.R. McVicar, and D.J. Barrett. Decomposition of vegetation cover into woody and herbaceous components using AVHRR NDVI time series. *Remote Sensing of Environment*, 86(1):1–18, 2003.

J. A. Ludwig, G. N. Bastin, V. H. Chewings, R. W. Eager, and A. C. Liedloff. Leakiness: A new index for monitoring the health of arid and semiarid landscapes using remotely sensed vegetation cover and elevation data. *Ecological Indicators*, 7(2):442–454, 2007.

S. R. Murphy and G. M. Lodge. Ground cover in temperate native perennial grass pastures. I. A comparison of four estimation methods. *The Rangeland Journal*, 24(2):288–300, 2002.

G. S. Okin, D. A. Roberts, B. Murray, and W. J. Okin. Practical limits on hyperspectral vegetation discrimination in arid and semiarid environments. *Remote Sensing of Environment*, 77(2):212–225, 2001.

P. O'Reagain, J. Bushell, C. Holloway, and A. Reid. Managing for rainfall variability: Effect of grazing strategy on cattle production in a dry tropical savanna. *Animal Production Science*, 49(2):85–99, 2009.

R. P. Pech, A. W. Davis, R. R. Lamacraft, and R. D. Graetz. Calibration of LANDSAT data for sparsely vegetated semi-arid rangelands. *International Journal of Remote Sensing*, 7(12):1729–1750, 1986a.

R. P. Pech, R. D. Graetz, and A. W. Davis. Reflectance modelling and the derivation of vegetation indices for an Australian semi-arid shrubland. *International Journal of Remote Sensing*, 7(3):389–403, 1986b.

S. Phinn, M. Stanford, P. Scarth, A. T. Murray, and P. T. Shyy. Monitoring the composition of urban environments based on the vegetation-impervious surface-soil (VIS) model by subpixel analysis techniques. *International Journal of Remote Sensing*, 23(20):4131–4153, 2002.

G. Pickup, G. N. Bastin, and V. H. Chewings. Identifying trends in land degradation in non-equilibrium rangelands. *Journal of Applied Ecology*, 35(3):365–377, 1998.

P. Puyou-Lascassies, G. Flouzat, M. Gay, and C. Vignolles. Validation of the use of multiple linear regression as a tool for unmixing coarse spatial resolution images. *Remote Sensing of Environment*, 49(2):155–166, 1994a.

P. Puyou-Lascassies, G. Flouzat, M. Gay, and C. Vignolles. Validation of the use of multiple linear regression as a tool for unmixing coarse spatial resolution images. *Remote Sensing of Environment*, 49(2):155–166, 1994b. ISSN 00344257.

T. W. Ray and B. C. Murray. Nonlinear spectral mixing in desert vegetation. *Remote Sensing of Environment*, 55(1):59–64, 1996.

D. A. Roberts, M. Gardner, R. Church, S. Ustin, G. Scheer, and R. O. Green. Mapping chaparral in the Santa Monica Mountains using multiple endmember spectral mixture models. *Remote Sensing of Environment*, 65 (3):267–279, 1998.

A. Röder, T. Kuemmerle, and J. Hill. Extension of retrospective datasets using multiple sensors. An approach to radiometric intercalibration of Landsat TM and MSS data. *Remote Sensing of Environment*, 95(2):195–210, 2005.

A. Röder, T. Kuemmerle, J. Hill, V. P. Papanastasis, and G. M. Tsiourlis. Adaptation of a grazing gradient concept to heterogeneous Mediterranean rangelands using cost surface modelling. *Ecological Modelling*, 204 (3-4):387–398, 2007.

A. Röder, J. Hill, B. Duguy, J. A. Alloza, and R. Vallejo. Using long time series of Landsat data to monitor fire events and post-fire dynamics and identify driving factors. A case study in the Ayora region (eastern Spain). *Remote Sensing of Environment*, 112(1):259–273, 2008a.

A. Röder, Th Udelhoven, J. Hill, G. del Barrio, and G. Tsiourlis. Trend analysis of Landsat-TM and -ETM+ imagery to monitor grazing impact in a rangeland ecosystem in Northern Greece. *Remote Sensing of Environment*, 112(6):2863–2875, 2008b.

R. Salvador and X. Pons. On the reliability of landsat TM for estimating forest variables by regression techniques: A methodological analysis. *IEEE Transactions on Geoscience and Remote Sensing*, 36(6):1888–1897, 1998.

P. Scarth and S. Phinn. Determining forest structural attributes using an inverted geometric-optical model in mixed eucalypt forests, Southeast Queensland, Australia. *Remote Sensing of Environment*, 71(2):141–157, 2000.

P. Scarth, M. Byrne, T. Danaher, B. Henry, R. Hassett, J. Carter, and P. Timmers. State of the paddock: monitoring condition and trend in groundcover across Queensland. In *13th Australasian Remote Sensing Conference*, Canberra, 2006.

E. Schlicht. Seasonal adjustment in a stochastic model. *Statistische Hefte*, 25(1):1–12, 1983. ISSN 00390631 (ISSN).

M Schmidt, P Scarth, and J Milne. Ground-cover estimation with iterative spectral mixture analysis. In E Edwards and R Bartolo, editors, *14th Australian Remote Sensing and Photogrammetry Conference*, Darwin, 2008.

J. Settle and N. Campbell. On the errors of two estimators of sub-pixel fractional cover when mixing is linear. 36(1):163–170, 1998. ISSN 0196-2892.

J. J. Settle. On the relationship between spectral unmixing and subspace projection. *IEEE Transactions on Geoscience and Remote Sensing*, 34(4):1045–6, 1996.

C. Small. The Landsat ETM+ spectral mixing space. *Remote Sensing of Environment*, 93(1-2):1–17, 2004. ISSN 00344257.

M. Stellmes, T. Udelhoven, A. Röder, and J. Hill. Dryland observation at local and regional scale - Comparison of Landsat TM and NOAA AVHRR time series. In *Proceedings of SPIE - The International Society for Optical Engineering*, volume 7104, Cardiff, Wales, 2008.

J. Wallace, G. Behn, and S. Furby. Vegetation condition assessment and monitoring from sequences of satellite imagery. *Ecological Management and Restoration*, 7(SUPPL. 1), 2006.

R. A. Washington-Allen, N. E. West, R. D. Ramsey, and R. A. Efroymson. A protocol for retrospective remote sensing-based ecological monitoring of rangelands. *Rangeland Ecology and Management*, 59(1):19–29, 2006.

D. L. Williams, S. Goward, and T. Arvidson. Landsat: Yesterday, today, and tomorrow. *Photogrammetric Engineering and Remote Sensing*, 72(10):1171–1178, 2006.

H. D. Williamson and D. J. Eldridge. Pasture status in a semi-arid grassland. *International Journal of Remote Sensing*, 14(13):2535–2546, 1993.

P. Xu. Truncated SVD methods for discrete linear ill-posed problems. *Geophysical Journal International*, 135 (2):505–514, 1998.